A R C H I V E S O F M E T A L L U R G Y A N D M A T E R I A L S
Volume 53 2008 Issue 4

M. ŁOMOZIK*, A. ZIELIŃSKA-LIPIEC**

MICROSCOPIC ANALYSIS OF THE INFLUENCE OF MULTIPLE THERMAL CYCLES ON SIMULATED HAZ TOUGHNESS IN P91 STEEL

MIKROSKOPOWA ANALIZA WPŁYWU WIELOKROTNYCH CYKLI CIEPLNYCH SYMULOWANEJ SWC STALI P91 NA JEJ WŁASNOŚCI PLASTYCZNE

The X10CrMoVNb 9.10 steel, known under the designation T/P91, has been characterized. That up-to-date steel is intended for long-lasting service at elevated temperatures and is used for welded structures in the power industry.

Due to the limited weldability of the P91 steel, which manifests itself by the necessity of preheating before welding and post-weld heat treatment of welded joints, examinations of the influence of welding thermal cycles on the toughness of coarse grained regions of the heat affected zone (HAZ) have been performed. The simulation technique was applied to produce the following coarse-grained HAZ regions: CGHAZ, ICCGHAZ and SRCGHAZ, the fine-grained FGHAZ region and the HAZ region subjected to a tempering cycle (temper-bead).

On specimens with the simulated HAZ regions the impact absorbed energy was determined, Vickers hardness was measured and metallographic microscopic examinations have been performed. The examination results are presented in the form of diagrams and photographs of microstructures. Because both the initial microstructure of the P91 steel and the microstructures produced by multiple welding thermal cycles have a needle like morphology, it was difficult to trace significant changes in the microstructure of simulated HAZ regions only by the light microscope. That is why a trial was undertaken to analyze the changes, which occur in the microstructure of the P91 steel, by the electron transmission microscope (TEM). The TEM examination made possible the clarification of a regularity concerning the absorbed energy and hardness dependence on the cooling time in the temperature range from 800 to 500 °C ($t_{8/5}$ cooling time), which is specially distinct in the SRCGHAZ range.

W artykule scharakteryzowano stal w gatunku X10CrMoVNb9.10 znaną pod oznaczeniem T/P91. Stal ta jest nowoczesną stalą przeznaczoną do długotrwałej eksploatacji w podwyższonych temperaturach i jest stosowana na spawane konstrukcje energetyczne.

W związku z ograniczoną spawalnością stali P91, która przejawia się koniecznością podgrzewania wstępnego stali przed spawaniem a następnie obróbki cieplnej gotowego złącza po spawaniu, przeprowadzono badania wpływu cykli cieplnych spawania na własności plastyczne gruboziarnistych obszarów strefy wpływu ciepła (SWC). Badania były prowadzone w oparciu o technikę symulacji i dotyczyły obszarów gruboziarnistych SWC: CGHAZ, ICCGHAZ i SRCGHAZ, obszaru o strukturze drobnoziarnistej FGHAZ oraz obszaru SWC poddanego oddziaływaniu cyklu cieplnego odpuszczającego (temper bead).

W dalszej kolejności na próbkach z symulowanymi obszarami SWC przeprowadzono badania pracy łamania, pomiary twardości oraz badania metalograficzne mikroskopowe. Wyniki tych badań przedstawiono w formie wykresów i zdjęć mikrostruktur. Ponieważ zarówno struktura wyjściowa stali P91, jak i struktury powstające w rezultacie oddziaływania wielokrotnych cykli cieplnych mają morfologię iglastą, trudno było prześledzić znaczące zmiany w mikrostrukturze symulowanych obszarów SWC tylko i wyłącznie przy użyciu mikroskopu świetlnego. Dlatego podjęto próbę przeanalizowania zmian zachodzących w mikrostrukturze stali P91 za pomocą transmisyjnego mikroskopu elektronowego (TEM). Badania przy użyciu mikroskopu elektronowego umożliwiły wyjaśnienie pewnej prawidłowości dotyczącej zależności pracy łamania i twardości od wartości czasu stygnięcia w zakresie temperatur od 800 do 500 °C (czas $t_{8/5}$), która jest szczególnie widoczna w obszarze SRCGHAZ.

* INSTITUTE OF WELDING, 44-100 GLIWICE, 16/18 BŁ. CZESŁAWA STR., POLAND
** AGH – UNIVERSITY OF SCIENCE & TECHNOLOGY, 30-059 KRAKÓW, 30 MICKIEWICZA AV., POLAND

1. Introduction

Changes which occur in the power industry stimulate the development of heat resistant steels. It is connected with the demand for materials which can operate at higher and higher temperatures (600 – 650 °C) and stresses (above 160 MPa). Only steels characterised by such parameters are suitable for the modernization of high rating power units or the manufacture of steam superheaters and resuperheaters as well as live steam pipes and turbine casings. The aforesaid requirements are best fulfilled by martensitic 9 to 12 % chromium steels with reduced carbon content (0.05 – 0.15 %), with molybdenum and tungsten additions and microalloyed with vanadium, niobium and nitrogen. By forming nitrides, MX type carbonitrides and $M_{23}C_6$ carbides, the components mentioned above increase the creep resistance of steels due to precipitation strengthening of material structure. The said group of steels also includes X10CrMoVNb 9.10 steel. It was developed in the 70's of the XX century and, acc. to ASTM, is known as T/P91. New martensitic steels are characterised first of all by a considerably higher creep strength allowing for lowering material consumption by reducing the thickness of wall of the structural element and thus giving evident economical and technical effects. One of important characteristics is good weldability of steel. The welding technology of P91 steel requires, however, a preheating temperature of ca. 200 °C as well as post-weld heat treatment (PWHT). The PWHT of P91 steel welded joint consists in relieving stress (i.e. tempering) within the temperature range of 730 – 750 °C; such processing results in obtaining very good toughness of weldment. The mechanical properties of the heat affected zone (HAZ) area are slightly lower, i.e. up to 20 % in comparison with those of the parent material. Tests reveal that the material decohesion occurs most often in the intercritically reheated area of the HAZ; temperature range being within $A_{C1} – A_{C3}$. For this reason, in order to determine the microstructure and properties of various areas of the zone, it was necessary to conduct a detailed comparative analysis on simulated HAZ's. The examination of microstructure is of particular interest as P91 steel is characterized by high hardenability making it possible to obtain martensitic microstructure on cross sections exceeding even 100 mm. In the as-delivery state, P91 steel has a microstructure of tempered martensite with elongated ferrite subgrains of high dislocation density and numerous $M_{23}C_6$ type carbides precipitated on subgrain boundaries as well as highly dispersive MX-type carbonitrides. Heating up to temperatures over A_{C1} leads to austenite formation, which during cooling transforms to martensite. Due to the needle-like morphology of both the initial and the newly formed microstructure, the use of a light microscope does not facilitate the evaluation of the changes of microstructure in that critical (from the properties' point of view) area of a welded joint. Therefore it proved necessary to use a transmission electron microscope TEM in order to analyse changes occurring in the microstructure.

2. Material used for examination and simulation programme

The chemical composition of X10CrMoVNb 9.10 (P91) martensitic steel is presented in TABLE 1

TABLE 1

Chemical composition of X10CrMoVNb 9.10 (P91) steel

Steel	Content of elements [%]										
	C	Mn	Si	P	S	Cr	Ni	Mo	V	$Al_{soluble}$	Nb
X10CrMoVNb 9.10	0.10	0.41	0.33	0.018	0.001	8.27	0.25	0.876	0.18	0.007	0.08
acc. to ASTM A335 [1]	0.08 ÷ 0.12	0.30 ÷ 0.60	0.20 ÷ 0.50	max 0.015	max 0.010	8.00 ÷ 9,50	max 0.40	0.85 ÷ 1.05	0.18 ÷ 0.25	max 0.04	0.06 ÷ 0.10

The temperatures A_{C1} = 800°C and A_{C3} = 890°C for P91 steel come from reference publications [2, 3].

Specimens for simulation of welding thermal cycles were machined from the tested steel. The specimen size and dimensions were the same as for notch toughness test (10 × 10 mm), which, following the simulation, facilitated their preparation for impact testing (Charpy V notch). A thermal- and strain cycle simulator was applied to simulate HAZ's areas of various microstructures and properties in the specimens affected by multiple welding thermal cycles. The following HAZ areas were simulated:

- **CGHAZ** (Coarse Grained HAZ) – HAZ area corresponding to coarse grained overheated zone,

- **FGHAZ** (Fine Grained HAZ) – HAZ area corresponding to fine grained zone, reheated to temperature exceeding A_{C3},
- **ICCGHAZ** (Intercritically Reheated Coarse Grained HAZ) – HAZ area corresponding to coarse grained zone reheated to intercritical temperatures $A_{C1} \div A_{C3}$,
- **SRCGHAZ** (Subcritically Reheated Coarse Grained HAZ) – HAZ area corresponding to coarse grained zone reheated to temperature below A_{C1},
- **After tempering cycle** (temper bead) – HAZ area corresponding to coarse grained overheated zone subjected to tempering cycle.

The simulation plan is presented in TABLE 2

TABLE 2

Parameters of welding thermal cycle simulation

Haz area	T_{max} / $T_{real.}$ [°C]			Cooling time $t_{8/5}$ [s] (*)		
	T_{max1}	T_{max2}	T_{max3}			
CGHAZ	1250/1252	–	–	6	24	60
FGHAZ	1250/1252	950/953	–			
ICCGHAZ	1250/1246	860/857	–			
SRCGHAZ	1250/1245	750/750	–			
After tempering cycle	1250/1250	790/790	550/553			

(*) $t_{8/5}$ – cooling time at the 800 ÷ 500 °C temperature range

3. Testing of impact strength, microstructure examination and hardness measurements of simulated HAZ areas

The specimens with simulated HAZ areas were used to conduct Charpy V notch toughness tests; the tests were performed at room temperature and in accordance with the requirements of standard PN-EN 10045-1 [4]. For every kind of welding thermal cycle, 5 specimens were impact tested. The two extreme absorbed energy values were rejected; the arithmetic mean was calculated on the basis of the three remaining values. The results are presented in Figures 7 ÷ 9.

From each series of specimens on which different welding thermal cycles were simulated, one specimen was selected for metallographic microscopic examination. Specimen surfaces, perpendicular to the surface with the machined Charpy V notch were polished for metallographic examination acc. to PN-EN 1321 standard [5]. The microstructures on P91 steel specimens were revealed by $FeCl_3$ etching. Examples of microscopic examination results of simulated HAZ's at the cooling time $t_{8/5}$ = 24 s and performed at the magnification of 1000×, are presented in Figures 1 ÷ 6 [6]. Afterwards, on the polished sections of the individual simulated HAZ's, Vickers hardness measurements were performed at the load of 9.807 N (HV1), acc. to the requirements of PN-EN ISO 6507-1 standard [7]. The results, as a mean value of 5 measurements, are presented in Figures 7 ÷ 9 [6].

As can be seen from Figures 7 ÷ 9, extension of the $t_{8/5}$ cooling time does not considerably lower hardness values. In case of the HAZ area reheated to a tempera-

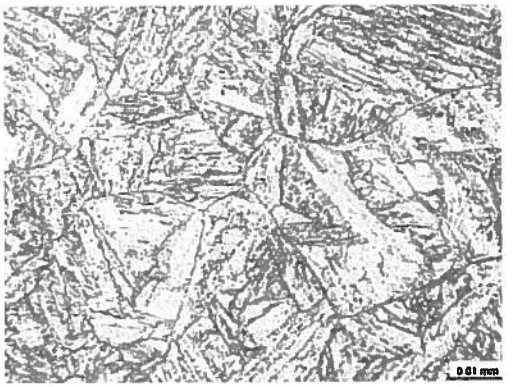

Fig. 1. Parent material of P91 steel. Tempered martensite (228 HV1)

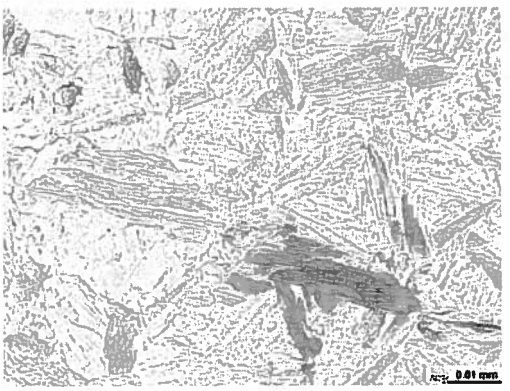

Fig. 2. Simulated HAZ area with coarse grained microstructure (CG-HAZ). Martensite (399 HV1)

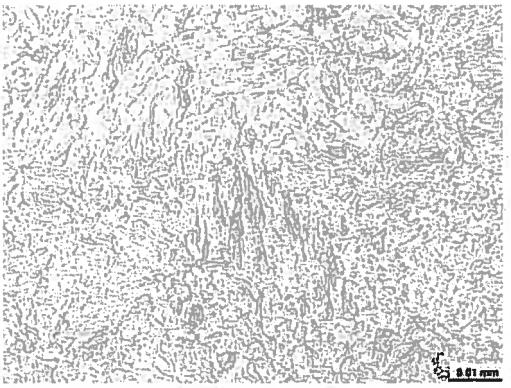

Fig. 3. Simulated HAZ area with fine grained microstructure (FGHAZ). Fine lamellar martensite (377 HV1)

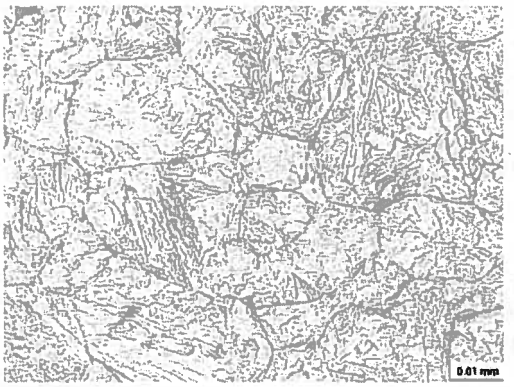

Fig. 4. Simulated HAZ area with coarse grained microstructure reheated to intercritical temperatures (ICCGHAZ; $A_{C1} < T_{max2} < A_{C3}$). Martensite (393 HV1)

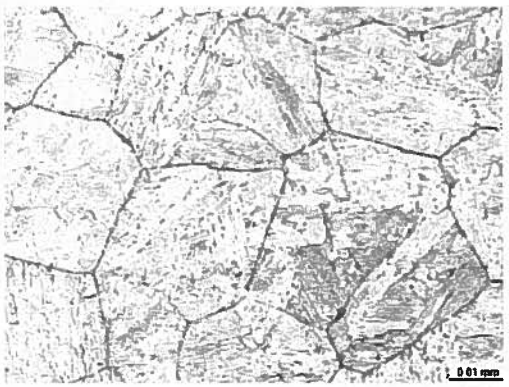

Fig. 5. Simulated HAZ area with coarse grained microstructure reheated to a temperature below A_{C1} (SRCGHAZ; $T_{max2} < A_{C1}$). Martensite + carbides precipitated on grain boundaries (373 HV1)

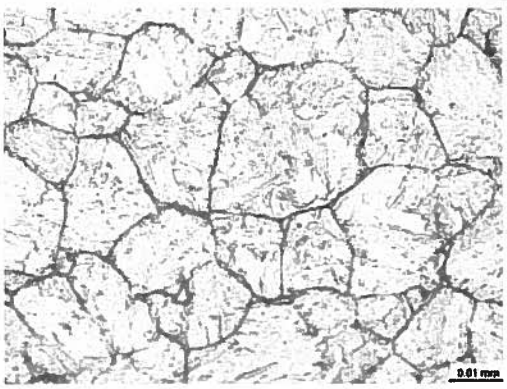

Fig. 6. Simulated HAZ area after tempering cycle (temper bead) ($T_{max2} < A_{C1}$ but close to A_{C1}, $T_{max3} < A_{C1}$). Martensite + carbides precipitated on grain boundaries (333 HV1)

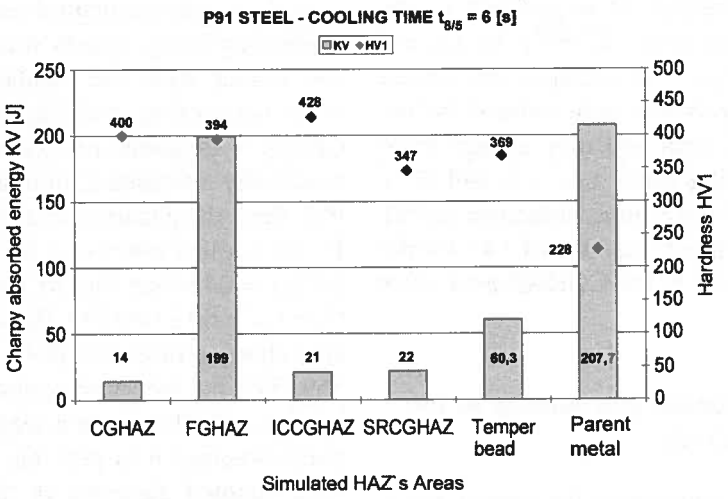

Fig. 7. Comparison of Charpy V absorbed energy KV and HV1 hardness of various HAZ areas simulated in P91 steel at the cooling time $t_{8/5}$ = 6 s

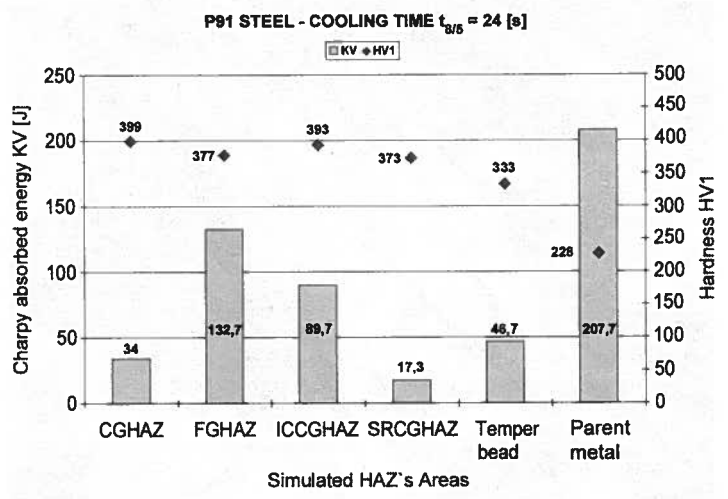

Fig. 8. Comparison of Charpy V absorbed energy KV and HV1 hardness of various HAZ areas simulated in P91 steel at the cooling time $t_{8/5}$ = 24 s

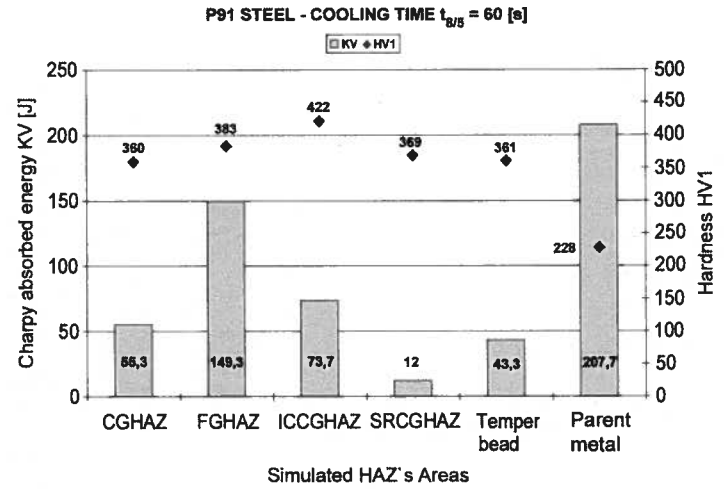

Fig. 9. Comparison of Charpy V absorbed energy KV and HV1 hardness of various HAZ areas simulated in P91 steel at the cooling time $t_{8/5}$ = 60 s

ture below A_{C1} (SRCGHAZ) it is possible to observe an increase in hardness from 347 HV1, for $t_{8/5}$ = 6 seconds, to 369 HV1, for $t_{8/5}$ = 60 seconds. The lowest Charpy V absorbed energy values were noticed for the coarse grained SRCGHAZ area and they change from 22 J to 12 J for the cooling times $t_{8/5}$ = 6 and 60 s respectively. Among all the HAZ areas simulated in P91 steel, the lowest absorbed energy was that of 14 J for the cooling time $t_{8/5}$ = 6 seconds, in the CGHAZ area, after a single thermal cycle.

4. Examination of martensite morphology in P91 steel [6]

Analysis of the results concerning the impact of $t_{8/5}$ cooling time on the Charpy V absorbed energy values of various microstructural areas of simulated HAZ's revealed regularity, which was especially evident for the SRCGHAZ area. The regularity shows that the increase of the $t_{8/5}$ cooling time is accompanied by the lowering of Charpy V absorbed energy, while the hardness remains practically unchanged. In case of the SRCGHAZ area of P91 steel, the absorbed energy KV is lowered from 22 J, for the cooling time $t_{8/5}$ = 6 s (see Fig. 7), through 17,3 J for $t_{8/5}$ = 24 s (see Fig. 8), down to 12 J, for the cooling time $t_{8/5}$ = 60 s (see Fig. 9), whereas the hardness of that area changes from 347 HV1, through 373 HV1 down to 369 HV1 for the same cooling times. After short single heating of P91 steel to a temperature of 1250 °C, in the microstructure it is possible to observe lath martensite with retained austenite in the form of films on grain boundaries (see Fig. 10 and 11).

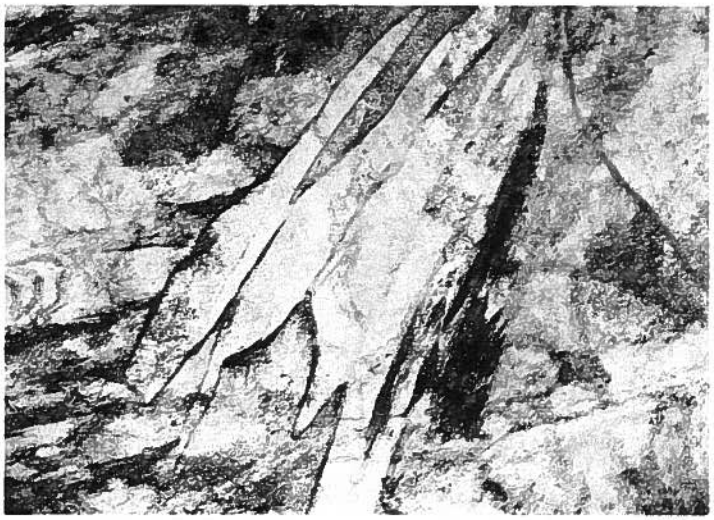

Fig. 10. CGHAZ area. Lath martensite with the remains of retained austenite in the form of films on grain boundaries

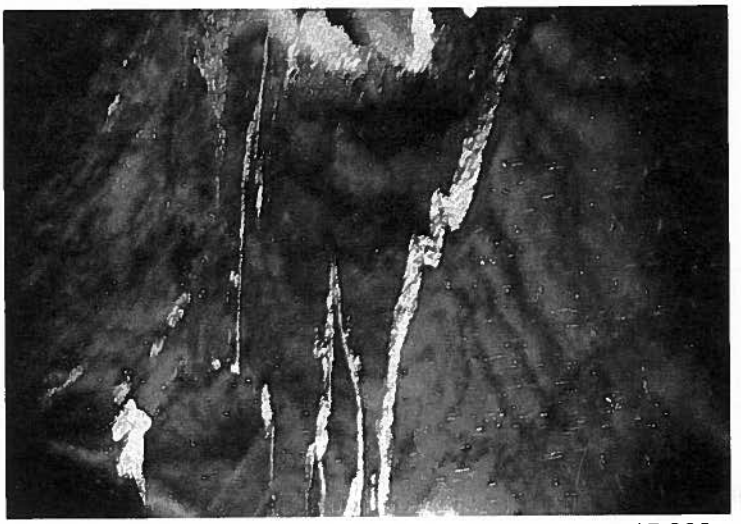

Fig. 11. CGHAZ area. Films of retained austenite visible in the dark field of the $[002]_\gamma$ reflex

The SRCGHAZ area has a heterogeneous microstructure, shown in Figure 12.

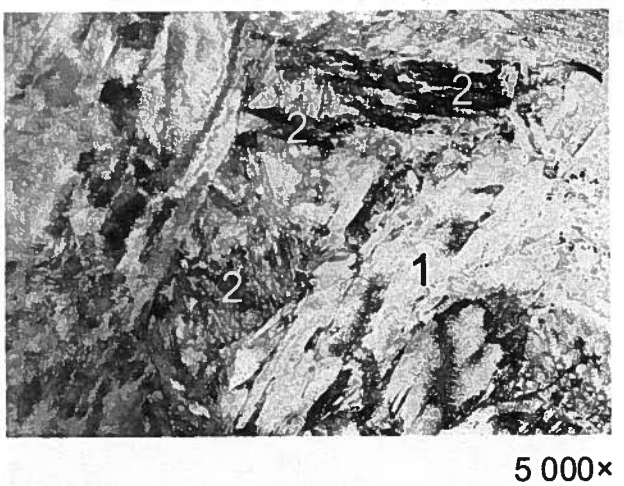

Fig. 12. Microstructure of P91 steel simulated by SRCGHAZ cycle: 1 – primary martensite, 2 – secondary martensite

In the steel microstructure two kinds of microstructure can be distinguished, depending on whether in the second thermal cycle martensite was transformed to austenite, or not. The fields in Fig. 12 marked by digit 1 are areas which were not transformed to austenite (primary martensite) during the second thermal cycle. They are characterised by lower dislocation density; the effects of the self-tempering process are visible in the form of M_3C type carbides (Fig. 13).

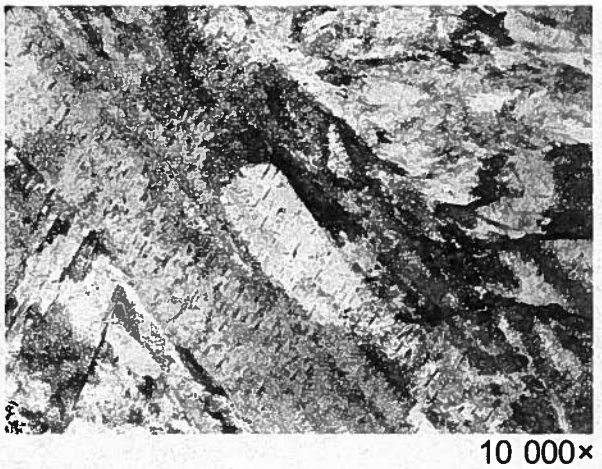

Fig. 13. Tempered martensite with M_3C carbides precipitated inside the laths

The fields marked by digit 2 were transformed into austenite during the first thermal cycle; during cooling they transformed again into needle-shaped fine lath martensite (secondary martensite).

The retained residual austenite, present on the martensite lath boundaries, is supersaturated with alloying elements. The SRCGHAZ area of P91 steel was obtained after a double thermal cycle; the second cycle heated the metal to a temperature below the critical temperature A_{C1}. During heating to the temperature below A_{C1}, carbides are precipitated both from martensite and retained austenite. Therefore, austenite is depleted on carbon and alloying elements. During cooling, such a destabilised martensite transforms to secondary martensite. Owing to the fact that the aforementioned austenite was rich in carbon, the newly formed martensite is characterised by low toughness, much lower than that of the primary tempered martensite. The microstructure of the SRCGHAZ area with the secondary martensite formed from the retained austenite after the second thermal cycle is presented in Figure 14.

The presence of microtwins in the martensite microstructure proves that the secondary martensite was formed from austenite with a high carbon content (see Figures 15 and 16).

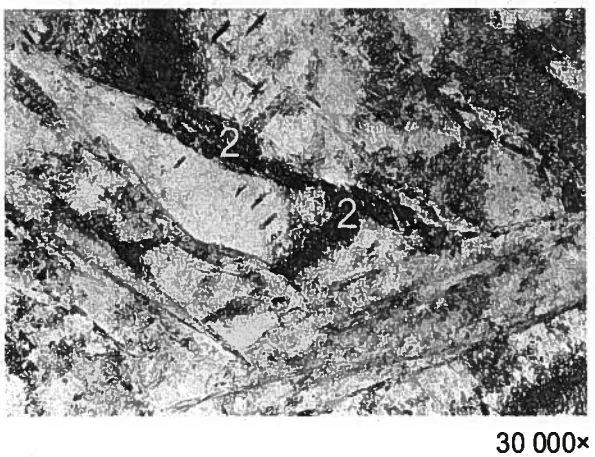

Fig. 14. SRCGHAZ area: 2 – secondary martensite

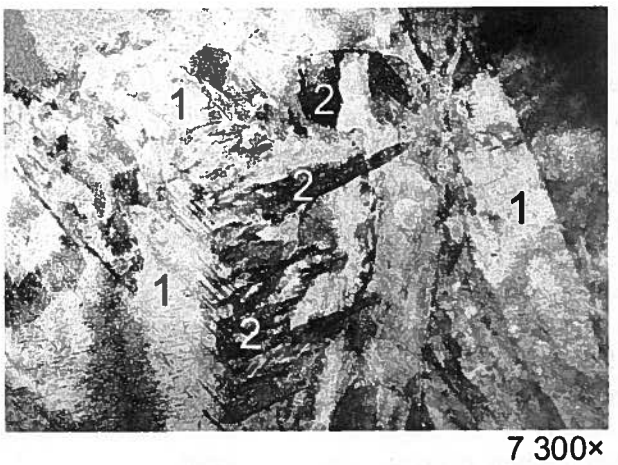

Fig. 15. Microstructure of P91 steel after simulation by the cycle SRCGHAZ: 1 – primary martensite, 2 – secondary martensite

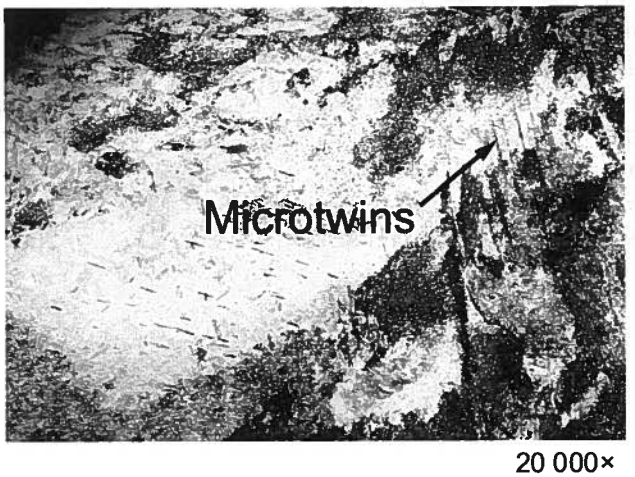

Fig. 16. SRCGHAZ area. Microtwins formed as a result of phase transformation of austenite to martensite

5. Summary

The analysis of the influence of $t_{8/5}$ cooling time on the hardness and Charpy V absorbed energy of HAZ areas simulated in P91 steel leads to the following conclusions:

- (a) cooling time extension does not cause any evident decrease in hardness of simulated HAZ areas;
- (b) fine grained HAZ area FGHAZ, obtained after a double thermal cycle with the maximum temperature of the second cycle higher than the critical temperature A_{C1}, is characterized by the highest impact absorbed energy values;
- (c) there is no explicit impact of cooling time on the Charpy V absorbed energy of coarse grained HAZ areas (ICCGHAZ and SRCGHAZ).

In order to conduct a detailed analysis of the observed changes of properties occurring in the HAZ simulated areas of P91 steel, and first of all, to clarify low toughness of the SRCGHAZ area, it was necessary to perform microstructure examinations by means of a light microscope as well as transmission electron microscope (TEM).

In the as-received conditions, prior to simulation, P91 steel has a microstructure of tempered martensite with elongated ferrite subgrains and high dislocation density in grain interiors, as well as numerous $M_{23}C_6$ carbides and MX type carbonitrides. The application of a short simulated thermal cycle as well as the chemical composition of the tested steel (alloy elements) are responsible for the fact that heating to a temperature slightly above A_{C3} does not lead to complete structural transformation of martensite to austenite. As a result, a heterogeneous microstructure is formed. The aforesaid structure is composed of fields of tempered martensite which was not structurally transformed during the heating as well as of the fields of the newly formed martensite produced from austenite formed during the heating process. The martensite which was not transformed during heating was called the primary martensite, while

the martensite formed in the steel microstructure during reheating – the secondary martensite. The examination results prove that privileged sites for austenite nucleation during heating are former austenite grain boundaries and lath pack boundaries of martensite. The most stable are the areas of the martensite which was self-tempered during the first heating cycle. The reheating of tested P91 steel to a temperature lower than A_{C3} results in the formation of a similar microstructure, where the fraction of secondary martensite decreases along with the lowering of the maximum temperature of a thermal cycle.

TEM examinations revealed that heating steel to a temperature range above A_{C1} results in austenite formation in the areas with higher carbon content, e.g. close to carbides. During cooling, the aforesaid austenite enriched in carbon transforms to twinned martensite (secondary martensite). In case of thermal cycles with maximum temperatures lower than A_{C1}, it is possible to observe thermal destabilization of retained austenite transforming to secondary martensite during cooling. The presence of twinned secondary martensite and fine-dispersed hardening precipitates (M_3C carbides) formed during the thermal cycle lead to a decrease in toughness of the HAZ areas where they appear (Figures 13 and 16).

Received: 17 March 2008.

REFERENCES

[1] ASTM A335. Seamless Ferritic Alloy Steel Pipe for High Temperature Service.
[2] The P91 Book. Ferritic pipe for high temperature use in boilers and petrochemical applications. Vallourec Industries, (1992).
[3] K. Haarmann, J. C. Vaillant, W. Bendick, A. Arbab, The T91/P91 Book. Vallourec & Mannesmann Tubes, (1999).
[4] PN-EN 10045-1:1994 Metallic materials. Charpy impact test. Part 1: Test method.
[5] PN-EN 1321:2000 Destructive tests on welds in metallic materials. Macroscopic and microscopic examination of welds.
[6] M. Łomozik, Examination of changes of HAZ properties in steels under the influence of multiple welding thermal cycles based on simulation technique. Research work of the Institute of Welding in Gliwice, No Id-115, (2003), (in Polish).
[7] PN-EN ISO 6507-1:2007 Metallic materials. Vickers hardness test. Part 1: Test method (ISO 6507-1:2005).